

Fully 3-D Printed Tunable Microwave Subsystem

Sang-Hee Shin^{#1}, Diyar Alyasiri^{#2}, Mario D'Auria^{#3}, William J. Otter^{#4}, Connor W. Myant^{*5},
Daniel Stokes⁺⁶, Zhengrong Tian⁺⁷, Nick M. Ridler⁺⁸, Stepan Lucyszyn^{#9}

[#] Department of Electrical and Electronic Engineering, Imperial College London, United Kingdom

^{*} Dyson School of Design Engineering, Imperial College London, United Kingdom

⁺Electromagnetic and Electrochemical Technologies Department, National Physical Laboratory, United Kingdom

{¹sanghee.shin11, ⁵connor.myant, ⁹s.lucyszyn}@imperial.ac.uk,
²diyaralyasiri@outlook.com, ³crisostomo231@yahoo.it, ⁴wjotter@gmail.com,
{⁶daniel.stokes, ⁷zhengrong.tian, ⁸nick.ridler}@npl.co.uk

Abstract — This paper introduces the first fully 3-D printed tunable microwave subsystem, consisting of 26 circuit elements. Here, a polymer-based 3-D printed Ku-band 4-element steerable phased-array antenna with fully integrated beam forming network is demonstrated. The measured radiation pattern revealed that the phased-array antenna subsystem has a total beam steering angle of 54°. This work clearly shows the potential of using 3-D printing technologies for manufacturing fully integrated subsystems with complex geometric features.

Keywords— Additive manufacturing, 3-D printing, Polyjet, fused deposition modeling (FDM), ABS, Ku-band, rectangular waveguide, phased-array antenna.

I. INTRODUCTION

Metal-pipe rectangular waveguides (MPRWGs) are widely used due to their low loss characteristics. However, as the structure gets smaller and more complicated, the manufacturing costs become a significant drawback. Over the past few years, various 3-D printing technologies have been studied as alternative fabrication methods for rectangular waveguides and other associated radio frequency components [1]-[7]. Polymer-based 3-D printing technologies allow significant reductions in fabrication time, weight and cost, while ensuring near-comparable RF performance to their conventionally machined counterparts.

With conventional MPRWGs, components are manufactured as separate components and assembled together to make a complete subsystem, requiring many waveguide flange connections; each contacting pair introducing a degradation in performance. In contrast, 3-D printing technologies allow more complex 3-D structures to be manufactured. Also, the number of parts can be significantly reduced with 3-D printing, minimizing the number of flanges. Polymer-based 3-D printing has been used to demonstrate relatively complex devices with repeating features, such as waveguide slot arrays [8] [9]. More complicated antenna arrays, which include components such as a flange, E-plane dividers and horn antennas, have been developed using stereolithography (SLA) [10].

This paper introduces the design and preliminary measured results of a fully 3-D printed 4-element steerable phased-array antenna subsystem. Here, 26 circuit elements (1 flange, 6 mitred bends, 3 power splitters, 4 tunable delay lines, 4 90°

waveguide twists, 4 bent interconnects and 4 H-plane sectoral horn antennas) are manufactured as a fully integrated, complete, subsystem. In addition, fully 3-D printed variable-position dielectric insertion mechanisms have been developed to implement tunable delay lines. All the measurements are performed by the UK's National Physical Laboratory, with reference to the UK's primary national measurement standards.

II. ANTENNA SUBSYSTEM DESIGN

The beamforming network and individual horn antennas have been designed as a fully-integrated phased-array subsystem. The subsystem consists of 7 different types of MPRWG components: flange, bends, power splitters, tuneable delay lines, twists, interconnects and horn antennas. All the waveguide components are based on conventional WR-62 waveguide, operating at Ku-band. The design has been optimized for operation between 15 and 17 GHz.

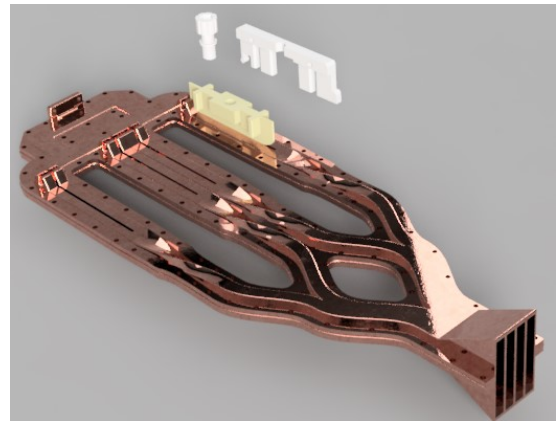


Fig. 1. CAD-rendered drawing of phased-array antenna subsystem design.

With the 4-element phased-array antenna having a single input waveguide port, three symmetrical power splitters were introduced to create a 4-way corporate feed. Independent tunable delay lines were integrated, followed by 90° twists. Bent waveguide interconnects were required to feed the individual H-plane sectoral horn antennas, while maintaining equal delay paths when there is no steering from broadside boresight. The distance between each horn was set to be 10 mm,

corresponding to half the free-space wavelength at 15 GHz. The CAD rendered drawing of the phased-array antenna with one dielectric insert is shown in Fig. 1.

The dielectric inserts were designed to fit through slots on the top walls of the waveguide. The concept was adopted from a previous X-band proof-of-principle design [7] and modified to provide better RF performance. To achieve the maximum relative phase shift, and minimum losses, the dielectric inserts were designed to have a rectangular shape with elliptically tapered edges on both front and rear ends. 3-D printed brackets were designed to have a 3-D printed calibrated screw mechanism that inserts and extracts the dielectric pieces linearly and evenly through the slots.

Electromagnetic (EM) simulations were performed using ANSYS HFSS to optimize the size and shape of the tapered edges of the dielectric inserts. Simulation results are shown in Fig. 2, which clearly show that the elliptical taper shape has superior return and insertion loss behavior across Ku-band. At 15 GHz, with the dielectric insert at maximum depth, a relative phase shift of 262° is predicted.

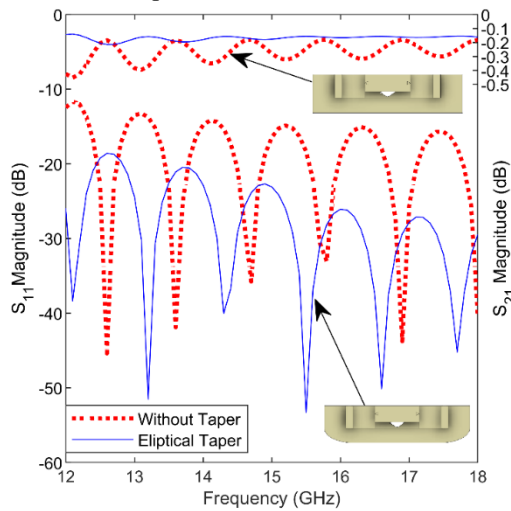
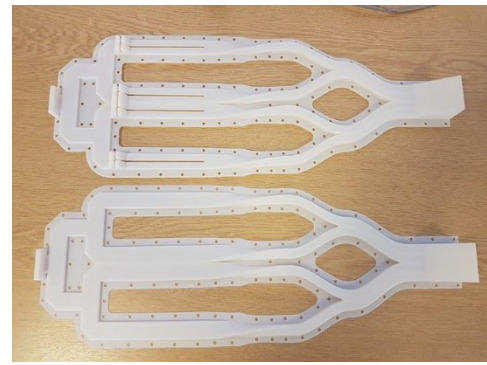


Fig. 2. Simulated S-parameters for the tunable delay line, with dielectric insert at maximum depth, without tapers (dotted red) and with elliptical tapers (solid blue).

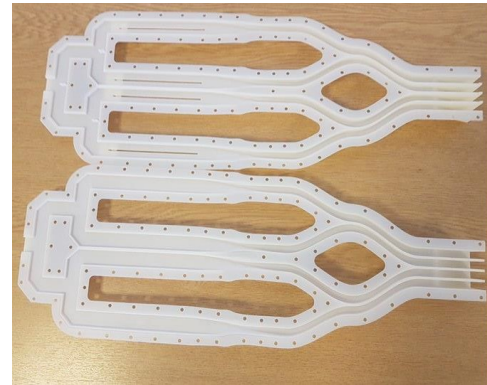
III. FABRICATION

A Polyjet 3-D printer (Stratasys Objet500 Connex3) was used for fabricating the MPRWG parts of the phased-array antenna subsystem. This printer is capable of printing large models at high resolution (maximum build area of $490 \times 390 \times 200 \text{ mm}^3$, with a minimum layer height of $16 \mu\text{m}$) by using its polymer jetting technology. The Polyjet printer jets photopolymer droplets that solidify when cured by an internal ultraviolet (UV) light source. It utilizes wax-like support material that allows the 3-D printer to print complex geometric features, such as curves and twists at the required resolution.

The main body of the phased-array antenna subsystem is printed in only two pieces. The support material was mechanically removed and cleaned with a high-pressure water jet, with the results shown in Fig. 3. After cleaning, a commercial electroplating metallization process was employed to give a $20 \mu\text{m}$ thick copper layer.



(a)



(b)

Fig. 3. A 3-D printed prototype before metallization: (a) external views; and (b) internal views.

Fused deposition modeling (FDM) 3-D printing was used to manufacture the dielectric inserts for the tunable delay lines, their mounting brackets and calibrated screw mechanism. The dielectric inserts were fabricated using an Ultimaker 2, with an acrylonitrile butadiene styrene (ABS) filaments. The brackets and screw mechanism were fabricated using an Original Prusa i3 MK3, with polylactic acid (PLA) filaments. The FDM parts were all lightly sanded-down to increase their smoothness for ease in assembly and operation.

IV. MEASUREMENTS

The input return loss and relative phase shift, for the complete phased-array antenna subsystem at boresight, were measured against dielectric insert depth. The phased-array antenna subsystem and receiving horn antenna were attached to fixed mounts with the boresight of the array aligned with the receiver horn. This measurement setup is shown in Fig. 4(a).

The measured results show that the return loss without any dielectric inserts is better than 12.9 dB across the operating frequency band (15-17 GHz). When the dielectric inserts are at maximum depth, the worst-case return loss is 16.3 dB. From measured insertion phase, a 263° maximum relative phase shift is achieved at 15 GHz, which is within 0.4 % of predictions.

The E- and H-plane radiation patterns of the phased-array antenna were measured using NPL's spherical test range. The phased-array antenna subsystem was mounted on a phi-over-theta spherical positioner, illustrated in Fig. 4(b), with its

aperture aligned over the rotation axis of the theta positioner. A WR-62 standard gain horn was used as the source antenna, which was installed on the polarization positioner. The separation distance between the source antenna and the phased-array antenna was 6 m.

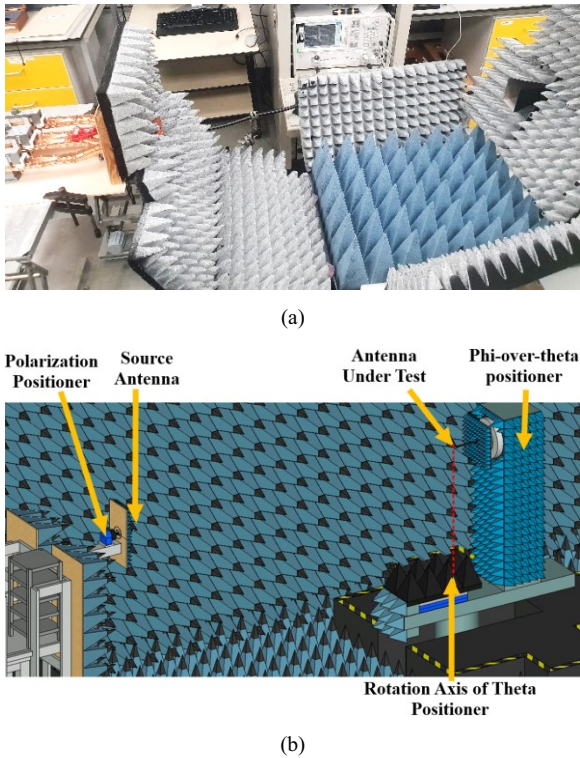


Fig. 4. NPL measurement setups: (a) VNA setup for return loss and phase shift at boresight; (b) Illustration of the anechoic chamber for measuring far-field radiation patterns.

Measured far-field E-plane radiation patterns are shown in Fig. 5. It can be seen that the total beam steering angle is 54° at 15 GHz. By controlling the dielectric insert penetration depth, the phased-array antenna's beam angle can be adjusted to scan between -27° and $+27^\circ$.

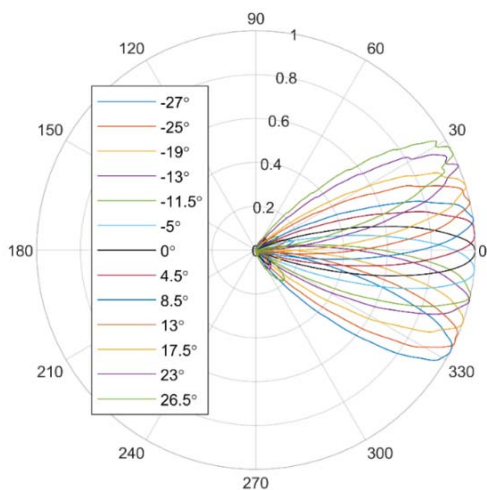


Fig. 5. Measured far-field E-plane radiation patterns at 15 GHz.

V. CONCLUSION

This paper introduces a fully 3-D printed tunable microwave subsystem. The Ku-band 4-element phased-array antenna was manufactured using polymer-based 3-D printing technologies, consisting of 26 circuit elements, and demonstrated excellent measured performance. By independently adjusting the depths of the dielectric inserts, the beam was fully steerable from -27° to $+27^\circ$ at 15 GHz. More in-depth simulations, measurements and analysis are currently being investigated. It is evident that 3-D printing technologies are capable of producing low-cost and high-performance devices, not only at component level but also at subsystems levels.

ACKNOWLEDGMENT

The authors would like to thank their colleague, Dr. X. Shang, at NPL, for arranging the electroplating.

REFERENCES

- [1] M. D'Auria, W. J. Otter, J. Hazell, B. T. W. Gillatt, C. Long-Collins, N. M. Ridler and S. Lucyszyn, "3-D printed metal-pipe rectangular waveguides", *IEEE Trans. on Components, Packaging and Manufacturing Technology*, vol. 5, no. 9, pp. 1339-1349, Sep. 2015.
- [2] W. J. Otter and S. Lucyszyn, "Printing: the future of THz," *IET Electronics Letters*, vol. 53, no. 7, p. 433, Mar. 2017.
- [3] W. J. Otter, N. M. Ridler, H. Yasukochi, K. Soeda, K. Konishi, J. Yumoto, M. Kuwata-Gonokami, and S. Lucyszyn, "3D printed 1.1 THz waveguides," *IET Electronics Letters*, vol. 53, no. 7, pp. 471-473, Mar. 2017.
- [4] S. Lucyszyn, X. Shang, W. J. Otter, C. Myant, R. Cheng, and N. M. Ridler, "Polymer-based 3D printed millimeter-wave components for spacecraft payloads," *IEEE MTT-S International Microwave Workshop Series on Advanced Materials and Processes (IMWS-AMP)*, Ann Arbor, USA, Jul. 2018 (Invited).
- [5] B. Al-Juboori, J. Zhou, Y. Huang, M. Hussein, A. Alieldin, W. J. Otter, D. Klugmann, and S. Lucyszyn, "Lightweight and low-loss 3-D printed millimeter-wave bandpass filter based on gap-waveguide", *IEEE Access*, vol. 7, no. 1, pp. 2624-2632, Jan. 2019.
- [6] W. J. Otter and S. Lucyszyn, "Hybrid 3-D-printing technology for tunable THz applications," *Proceedings of IEEE*, Special Issue on Additive Manufacturing of Radio-Frequency Components, vol. 105, no. 4, pp. 756-767, Apr. 2017.
- [7] B. T. W. Gillatt, M. D'Auria, W. J. Otter, N. M. Ridler, and S. Lucyszyn, "3-D printed variable phase shifter," *IEEE Micro. and Wireless Comp. Lett.*, vol. 26, no. 10, pp. 822-824, Oct. 2016.
- [8] G. P. L. Sage, "3D printed waveguide slot array antennas," *IEEE Access*, vol. 4, pp. 1258-1265, Mar. 2016.
- [9] G. McKerricher, A. Nafe, and A. Shamim, "Lightweight 3D printed microwave waveguides and waveguide slot antenna," *2015 IEEE International Symposium on Antennas and Propagation & USNC/URSI National Radio Science Meeting*, Vancouver, Canada, 2015, pp. 1322-1323.
- [10] B. Rohrdantz, C. Rave and A. F. Jacob, "3D-printed low-cost, low-loss microwave components up to 40 GHz," *2016 IEEE MTT-S International Microwave Symposium (IMS)*, San Francisco, USA, 2016, pp. 1-3.